

184-29155

THE STRUCTURE OF EVAPORATING AND COMBUSTING SPRAYS:
MEASUREMENTS AND PREDICTIONS

Semi-Annual Status Report
for the Period
January 1, 1984 to June 30, 1984

by

J-S. Shuen, A.S.P. Solomon and G. M. Faeth
Department of Mechanical Engineering
The Pennsylvania State University
University Park, Pennsylvania 16802

Prepared for

National Aeronautics and Space Administration
Grant No. NAG 3-190
NASA Lewis Research Center
R. Tacina, NASA Scientific Officer

July 1984

TABLE OF CONTENTS

	<u>Page</u>
NOMENCLATURE.	iii
SUMMARY	1
1. Introduction.	2
2. Theoretical Methods	4
2.1 General Description.	4
2.2 Locally Homogeneous Flow Model	5
2.3 Deterministic Separated Flow Model	6
2.4 Stochastic Separated Flow Model.	10
3. Experimental Methods.	11
3.1 Test Arrangement	11
3.2 Instrumentation.	14
3.3 Drop-Life-History Calibrations	15
4. Results and Discussion.	15
4.1 Drop-Life-History Calibrations	15
4.2 Monodisperse Spray Structure	18
5. Status and Plans for the Next Report Period	22
REFERENCES.	27

NOMENCLATURE

<u>Symbol</u>	<u>Description</u>
d	injector diameter
d_p	drop diameter
f	mixture fraction
g	square of mixture fraction fluctuations
k	turbulence kinetic energy
\dot{m}_O	injector flow rate
\dot{M}_O	injector thrust
$P(f)$	probability density function of f
Re	Reynolds number
r	radial distance
t	time
T	gas temperature
u	axial velocity
v	radial velocity
w	tangential velocity
x	axial distance
α	weighting factor for property selection
ϵ	rate of dissipation of turbulence kinetic energy
ρ	density
ϕ	fuel equivalence ratio

Superscripts

c	centerline quantity
p	drop property
0	injector exit condition
∞	ambient condition

Superscripts

()'	time-averaged fluctuating quantity
()"	Favre-averaged fluctuating quantity
($\bar{}$)	time-averaged mean quantity
($\tilde{}$)	Favre-averaged mean quantity

Semi-Annual Status Report
January 1, 1984 to June 30, 1984
The Structure of Evaporating and Combusting Sprays:
Measurements and Predictions

SUMMARY

This report describes progress on an investigation of spray structure for the semi-annual period January 1, 1984 to June 30, 1984. The objective of the work is to complete new measurements of the structure of particle-laden jets, nonevaporating sprays, evaporating sprays and combusting sprays. In addition to providing direct information on the structure of these flows, measurements have been completed in order to provide results useful for evaluation of models of these processes. Model evaluation is also being initiated, considering methods typical of current practice.

Work completed prior to this report period included particle-laden jets, nonevaporating sprays and evaporating sprays. Work during this report period concentrated on combusting sprays. This included development of an apparatus to allow observations of monodisperse sprays, initiation of measurements with this apparatus, calibration tests and analysis of single drop-life histories, and extension of prior analysis to consider combusting sprays.

The test arrangements consists of a methane-fueled turbulent jet diffusion flame with monodisperse methanol drops injected at the burner exit. Measurements were made of mean and fluctuating-phase velocities, drop sizes, drop-mass fluxes and mean-gas temperatures. Initial drop diameters of 100 and 180 microns are being considered in order to vary drop penetration in the flow and effects of turbulent dispersion. Baseline tests of the burner flame with no drops present were also conducted. Calibration tests, needed to establish methods for predicting drop transport, involved drops supported in the post-flame region of a flat-flame burner operated at various mixture ratios.

Spray models which are being evaluated include: (1) locally homogeneous flow (LHF) analysis, where interphase transport rates are assumed to be infinitely fast; (2) deterministic separated flow (DSF) analysis, where finite interphase transport rates are considered but effects of turbulence/drop interactions are ignored; and (3) stochastic separated flow (SSF) analysis, where both finite interphase transport rates and turbulence/drop interactions are considered using Monte Carlo methods. In all cases, analysis of the continuous phase uses a Favre-averaged $k-\epsilon-g$ turbulence model with the laminar flamelet technique for relating scalar properties to the local concentration of fuel species (the mixture fraction).

Baseline comparison between predictions and measurements was completed for drop-life histories and the turbulent burner flame which

suggest good performance for the methods used here. Tests have largely been completed for the 180 micron drop diameter spray and a portion of the test results are presented. The findings suggest significant effects of finite interphase transport rates, coupled with significant turbulent dispersion as the drops become small due to evaporation. Definitive analysis of this condition must await complete specification of burner exit conditions with measurements that are currently in progress.

Current work involves completing measurements of initial conditions for both combustor sprays and the structure of the 100 micron diameter monodisperse spray. Evaluation of all three models with the new data base will also be completed and all results reported during the next report period.

1. Introduction

The potential value of rational design procedures for liquid-fueled combustors has motivated numerous efforts to develop reliable models of spray evaporation and combustion. The goal is to reduce the time and cost of cut-and-try combustor development by providing a better understanding of fundamental spray processes and methods for estimating the effect of specific design changes. Numerous spray models have been proposed and some are already being used in industry to assist combustor development [1,2].* Nevertheless, there are few measurements available to evaluate model predictions and, as a consequence, no existing model has achieved a capability for reliable a priori predictions of spray properties. Therefore, the primary objective of the present investigation is to provide new experimental results for sprays in order to help fill this gap in the literature. A secondary objective is to initiate model evaluation--considering methods representative of current spray models.

New measurements are limited to steady axisymmetric flow configurations with flows injected into a stagnant air environment, to simplify both measurements and analysis. Experiments and theory are considering the following flows in turn:

- (1) Isothermal air jet--to establish theoretical and experimental methods by comparison with extensive results in the literature.
- (2) Particle-laden jets--to test effects of turbulent particle dispersion for a simple monodisperse two-phase flow.
- (3) Non-evaporating sprays--to provide a heavily loaded, polydisperse spray with high rates of flow deceleration typical of practical sprays.

*Numbers in brackets denote references.

- (4) Evaporating sprays--to test effects of interphase mass and energy transport.
- (5) Combusting gas jets--to establish a single-phase baseline for measurements and predictions of combusting flows.
- (6) Combusting monodisperse sprays--to study turbulence/drop interactions for a well-defined spray having properties similar to practical combustion chamber conditions.

In all cases, initial conditions are carefully defined, to allow definitive evaluation of analysis, since this was a major deficiency of past work. Measurements include: mean and fluctuating-phase velocities, mean particle (drop) mass fluxes, particle (drop) sizes, mean species concentrations and mean temperature--to the extent appropriate for each flow. Limitations of instrumentation, however, confined measurements to dilute portions of the multiphase flows, where void fractions were greater than 99%.

Three models of the process are being evaluated: (1) a locally homogeneous flow (LHF) model, where interphase transport rates are assumed to be infinitely fast; (2) a deterministic separated flow (DSF) model where finite interphase transport rates are considered, but effects of turbulence on interphase transport rates and particle dispersion are ignored; and (3) a stochastic separated flow (SSF) model where effects of finite interphase transport rates, turbulent dispersion and effects of turbulence on interphase transport rates are considered using random sampling for turbulence properties in conjunction with random-walk computations for particle motion. All three models use a $k-\epsilon-g$ turbulence model for the continuous phase, which was extensively evaluated in single-phase flows during earlier work in this laboratory and elsewhere. Theory has been evaluated using both data in the literature and the new data generated during the current investigation. Similar to the measurements, analysis was limited to dilute multiphase flows.

Prior to this report period, work was completed for the isothermal air jet, particle-laden jets, nonevaporating sprays and evaporating sprays. Full details of this work including comparison between predictions and measurements, are reported in earlier reports and papers prepared during this investigation [1-13]. Assessment thus far indicates that the LHF and DSF methods of analysis have limited utility for practical sprays, since effects of finite interphase transport rates and turbulence particle (drop) interactions are generally important. In contrast, the SSF approach, yielded more promising results and appears to be worthy of further development. A useful aspect of the current SSF method is that it requires only a modest increase in empiricism from turbulence models used to treat single-phase flows and is capable of treating nonlinear interactions between drops and turbulent fluctuations--at least to the extent that unit interphase processes are currently understood. Extension of these methods to dense sprays, where drop interactions with nearby drops, drop collisions, drop formation and direct effects of drops on

turbulence properties (called turbulence modulation) must still be addressed. Furthermore, performance of the method in dilute combusting sprays is still unknown. Due to current limitations on instrumentation, the present study has deferred consideration of dense sprays and is concentrating on dilute combusting sprays.

The objective of the present phase of the investigation was to consider dilute combusting sprays. Consideration of a monodisperse spray provides a simply characterized system, with well-defined initial conditions, and capabilities for concise presentation of findings. Test conditions have been chosen to maximize drop/turbulence interactions in a combusting environment since this is the major uncertainty in extending earlier analysis for noncombusting sprays. During this report period, the test apparatus was developed and measurements of spray structure were initiated. Methods for treating unit drop processes were evaluated, using auxiliary experiments. Finally, all three models were extended to treat combusting sprays.

Activities during the current report period are described in the following. The report begins with a description of theoretical and experimental methods. Some representative results concerning unit drop processes and spray structure are then described. The report concludes with a summary of current status and plans for the next report period in order to complete the study.

2. Theoretical Methods

2.1 General Description

Three theoretical models of spray processes are being considered: (1) a locally homogeneous flow (LHF) model, where slip between the phases is neglected and the flow is assumed to be in local thermodynamic equilibrium; (2) a deterministic separated flow (DSF) model, where slip and finite interphase transport rates are considered but effects of particle/drop dispersion by turbulence and affects of turbulence on interphase transport rates are ignored; and (3) a stochastic separated flow (SSF) model, where effects of interphase slip, turbulent dispersion and turbulent fluctuations are considered using random sampling for turbulence properties in conjunction with random-walk computations for particle motion. All three models use a $k-\epsilon-g$ turbulence model.

The theoretical models have been extensively described during earlier reports and papers emanating from this investigation [1-13] as well as earlier work in this laboratory [14-16]. Therefore, the models will only be described very briefly in the following in order to qualitatively indicate their features. Original references should be consulted for further details.

All models employ the widely adopted procedures of $k-\epsilon-g$ turbulence models for the gas phase, since this approach has been thoroughly calibrated during earlier work in this laboratory [1-16].

Major assumptions for the gas phase are: exchange coefficients of all species and heat are the same, buoyancy only affects the mean flow, and kinetic energy and radiative heat losses are negligible. Effects of buoyancy and radiation heat losses are generally small in practical sprays; therefore, treating these phenomena as perturbations is justified. Neglecting kinetic energy limits the model to low Mach number flows, which is appropriate for the test conditions to be examined as well as for the most practical combustion chambers. The assumption of equal exchange coefficients is widely recognized as being acceptable for high Reynolds number turbulent flows typical of spray processes.

The original formulation of the continuous phase was based on a time (Reynolds)-averaged formulation due to Lockwood and Naguib [17]. Recently, however, variable-density effects have been treated more concisely using mass weighted (Favre)-averages as suggested by Bilger [18]. The new approach has been examined for a series of turbulent jet flames of methane and propane burning in air [19]. The results indicate that Favre-averaging provides a unified treatment of constant and variable density turbulent jets with a single set of turbulence model constants.

Activities during the current report period are described in the following. The report begins with a description of theoretical and experimental methods. Some representative results concerning unit drop processes and spray structure are then described. The report concludes with a summary of current status and plans for the next report period in order to complete the study.

In order to ensure adequate numerical closure with reasonable computation costs, the model is limited to boundary-layer flows with no recirculation. The present test flows are axisymmetric with no swirl; conditions is that they correspond to cases where the turbulence models were developed and have high reliability.

2.2 Locally Homogeneous Flow Model

The governing equations for the LHF model are presented elsewhere [10-13]. The basic premise of this model is that rates of transport between phases are fast in comparison to the rate of development of the flow as a whole. This implies that all phases have the same velocity and temperature and that phase equilibrium is maintained at each point in the flow. Therefore, the LHF model implies that the process is mixing-controlled. The dispersed phase must have infinitely small particle sizes for this model to be exact. In practice, the model yields reasonably good results for finite-size particles having diameters less than 10 microns [1].

Under the LHF approximation, the flow is equivalent to a single-phase flow and effects of the dispersed phase only appear in the representation of thermodynamic properties (temperature, density, enthalpy, etc.) and molecular transport properties (viscosity, thermoconductivity, etc.). The representation of these properties is

generally called the state relationships for the flow. Finding state relationships for thermodynamic properties is relatively straightforward when the system is noncombusting, e.g., an evaporating spray. This involves conventional adiabatic mixing calculations with the local state of the mixture specified by the mixture fraction (the fraction of material at a point which originated at the injector) and the injector exit and ambient conditions.

When combustion is involved, extending state relation calculations to adiabatic flame calculations is straightforward, but tends to yield errors at high mixture fractions where low temperatures prevent equilibration. One tactic that has proved successful in this case involves the laminar flamelet method proposed by Bilger [20] and Liew et al. [21]. This follows from the observation that scalar properties in laminar flames are primarily functions of mixture fraction--relatively independent of length scales and flame stretch. Then measurements of scalar properties in an analogous (having the same boundary conditions) laminar flame yields a direct correlation of the state relationships assuming that turbulent flames are simply a succession of distorted laminar flamelets. Use of this approach for methane and propane fueled turbulent diffusion flames has proven to be successful and has been adopted for present work [22,23].

An example of the state relationships found in this manner for methane flames appears in Figs. 1 and 2, cf., Jeng and Faeth [22] for data sources. In spite of very different laminar flame conditions, it is seen that all the data yields very nearly universal correlations of scalar properties as a function of mixture fraction. An alternative procedure, useful in the many instances where laminar flame data is not available, is also illustrated in Figs. 1 and 2. This involves adiabatic flame calculations up to a critical fuel equivalence ratio (1.2 has been found to work best) followed by adiabatic mixing calculations at higher mixture fractions [22].

The main advantage of the LHF model is that there are only a few empirical constants, which are specified from earlier measurements, and only routine measurements in laminar flames are needed to find state relationships. Furthermore, only simplified injector quantities are required. The main defect is that the rate of flow development is overestimated in the two-phase region [1]. Nevertheless, potential users of spray models are likely to begin with a version of this type, since computations are no more difficult than for a single-phase flow. Therefore, it is desirable to evaluate its performance using the present experiments.

2.3 Deterministic Separated Flow Model

The deterministic separated flow model adopts the main features of the LHF model, but only for the gas phase. The liquid phase is treated by solving the Lagrangian equations of motion for the drops and then computing source terms in the governing equations for the gas phase which result from interphase transport effects. This general procedure corresponds to the particle tracking or

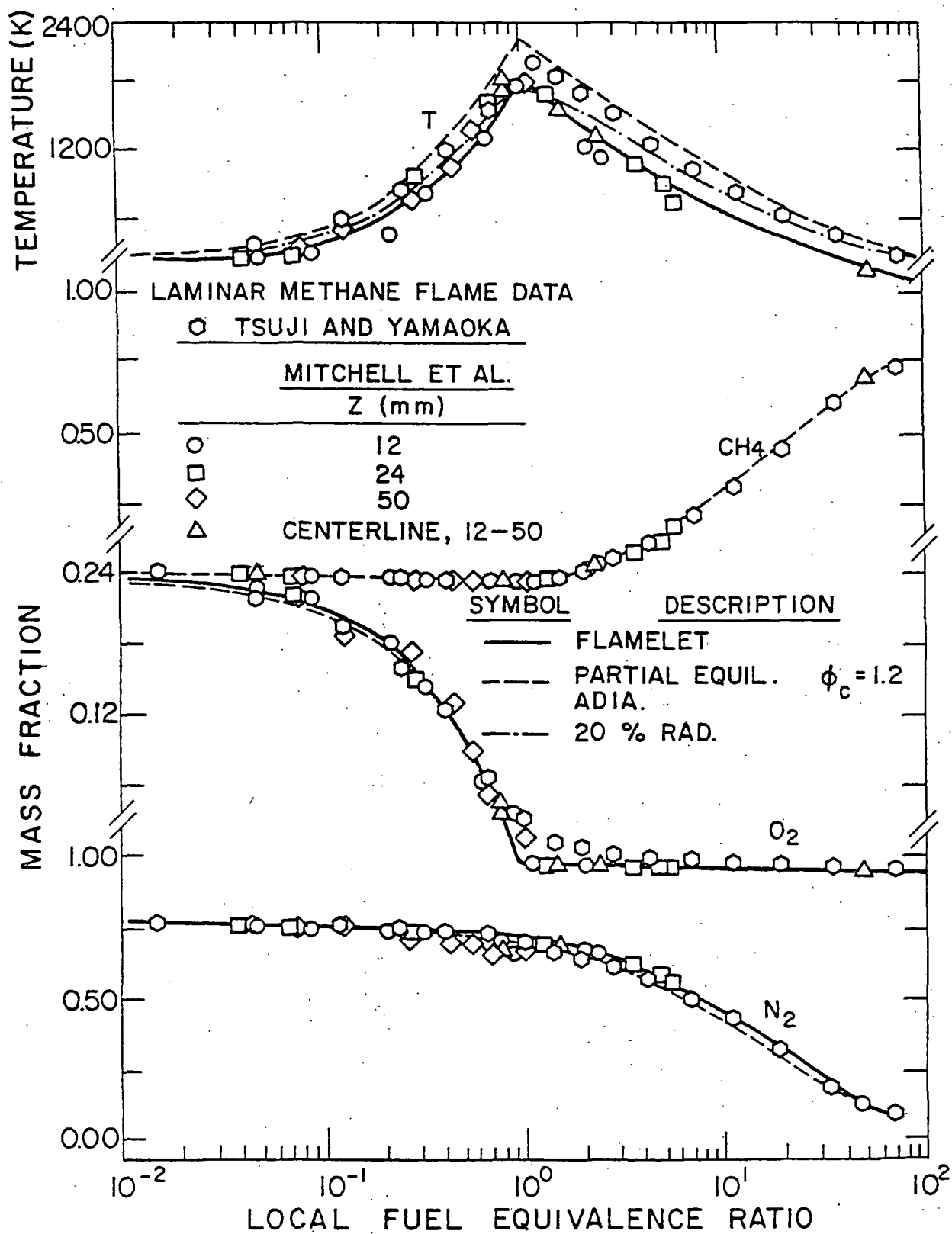


Fig. 1. State relationships for methane diffusion flames burning in air at normal temperature and pressure.

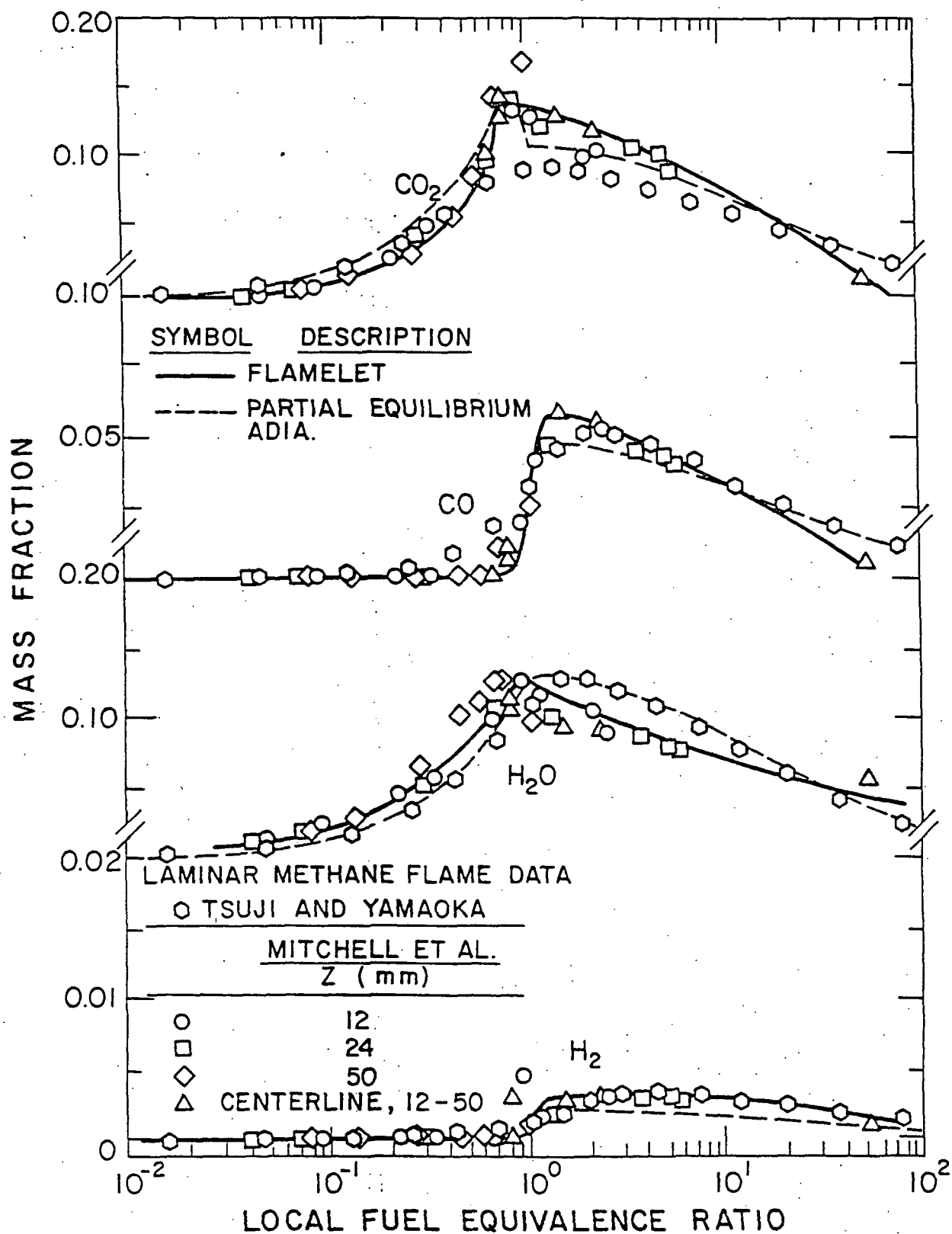


Fig. 2. State relationships for methane diffusion flames burning in air at normal temperature and pressure.

particle-source-in-cell methods used in most recent two-phase flow models. The approach is often called the discrete droplet model.

The main assumptions of the drop-trajectory calculations are as follows: dilute spray with drop-transport parameters equivalent to a single drop in an infinite environment; ambient conditions given by mean-flow properties; negligible effect of turbulent fluctuations on drop transport rates; empirical treatment of drag and convection effects; quasisteady gas phase; negligible shattering and collisions; liquid surface in thermodynamic equilibrium; and negligible radiation, Dufour and Soret effects. These assumptions are common for most spray models--their justification is discussed elsewhere [1,2].

Due to the difficulty of completely modeling internal transport processes of drops, an "onion skin" approximation has been adopted since past work suggests that this is a reasonable approximation for drop properties with good computational efficiency [1,16]. This involves the assumption that the drop surface adapts immediately to changes in local ambient conditions, while the bulk liquid remains at its initial state.

A key issue with respect to combusting sprays concerns the presence or absence of envelope flames around individual drops [1]. This is being examined during the present study since drops penetrate the flame zone and reach regions where oxygen is present in a relatively high temperature gas. The specification of ignition for drops in these circumstances is unknown at present; therefore, two limits are being examined: (1) ignoring envelope flames in all regions of the flow, and (2) assuming an envelope flame is present whenever the local environment contains oxidant. Past work in this laboratory suggests that differences between these limits are not large until the local fuel equivalence ratio drops below 0.8 [24].

Initial conditions for this model are defined at a position where drop size and velocity data can be obtained which is at the burner exit for present tests. Needed initial conditions are size, velocity, direction and number flux at various radial positions in the flow for the drops as well as velocities and turbulence properties of the continuous phase. At this position the drops are divided into n groups defined by their initial properties. Subsequent properties for each group are found by integrating governing conservation equations for momentum, energy, mass and velocity. During these computations, the properties of the continuous phase are taken to be mean properties found from the k - ϵ - g model. The interaction between the liquid and gas phases yields additional source terms for the continuous phase. These terms are found by computing the net change of mass, momentum and energy of each drop class as it crosses a computational cell. This procedure allows for full interaction between the phases, which is vital for treating the near-injector region.

The gas-phase equations are solved in the same manner as the LHF model. The only change in this portion of the program involves addition of the new source terms. The particle motion equations are

solved at the same time in a step-wise fashion, using a second-order finite difference algorithm.

2.4 Stochastic Separated Flow Model

The basic separated flow analysis considered in Section 2.3 only provides for deterministic trajectories of drop groups. In practical turbulent flows, however, drops are also dispersed by turbulent fluctuations. Furthermore, interphase-transport rates are influenced by fluctuations in local flow properties. These effects are considered in the stochastic separated flow model described in this section. The approach used to handle turbulent drop dispersion adapts stochastic methods first proposed by Gosman and Ioannides [25]. A complete discussion of the method appears in Refs. 1-13.

The stochastic separated flow model involves computing the trajectories of a statistically significant sample of individual drops as they move away from the injector (or the initial condition) and encounter a random distribution of turbulent eddies. These computations are completed using Monte Carlo methods. The main elements of this approach are methods for specifying the properties of each eddy and for determining the time of interaction of a particular drop with a particular eddy. The k - ϵ - g representation of turbulence is used in the SSF model to provide a convenient method for prescribing these properties.

Properties within a particular eddy are assumed to be uniform, but properties change in a random fashion from eddy to eddy. The computations for the continuous phase and the trajectory calculations are the same as the deterministic separated flow model. The main difference in the trajectory calculations is that mean-gas properties in these equations are replaced by the instantaneous properties of each eddy.

The properties of each eddy are found at the start of interaction by making a random selection from the probability density function of velocity and mixture fraction assuming that these properties are statistically independent. The velocity fluctuations are assumed to be isotropic with a Gaussian probability density distribution having a standard deviation obtained from the turbulence kinetic energy computed in the k - ϵ - g model. The cumulative distribution function for the three velocity components is formed and each distribution is randomly sampled. This involves selecting three numbers in the range 0-1 in computing the velocity components at these three values of the cumulative distribution function.

Instantaneous physical properties for each eddy are found in a similar manner. The instantaneous mixture fraction is assumed to have a clipped Gaussian probability density function with mean value and variance equal to \bar{f} and g . The cumulative distribution function is constructed for this PDF and a single random number selection in the range 0-1 yields the instantaneous mixture fraction of the eddy at the sample value of the cumulative distribution function. The state

relationships then provide the physical properties of the eddy at this mixture fraction. In this case state relationships are formed allowing only for the mixture fraction of the gas phase.

A drop is assumed to interact with an eddy for a time which is the minimum of either the eddy lifetime or the transit time required for the drop to cross the eddy. These times are estimated using the dissipation length scale and velocity fluctuation of the eddies. These parameters can be found directly from the $k-\epsilon$ -g model of the continuous phase.

The remainder of the computation proceeds similar to the deterministic separated flow model. The only change is that the source terms are computed for the random-walk trajectories of the particles as opposed to their deterministic solution. The main disadvantage of the stochastic method is that more particle trajectories must be considered in order to obtain statistically significant particle properties.

The stochastic model yields estimates of both mean and fluctuating particle properties at each point in the flow. This information is useful, since these properties can be measured and provide a good test of model performance. A notable feature of the model is that added empiricism is minimal--in fact, no new constants must formally be prescribed. The method has been extended to consider source terms due to particle interactions in the governing equations for turbulence quantities (called turbulence modulation). These effects are small, in present flows, however, since the sprays are very dilute [7-13].

Preliminary evaluation of the SSF model is described in Refs. 1-13. Flows considered included particle-laden jets, nonevaporating sprays and evaporating sprays. Comparison between predictions and measurements was very encouraging. However, uncertainties in initial conditions for many of the jet flows limited the thoroughness of this evaluation.

3. Experimental Methods

3.1 Test Arrangement

A sketch of the test apparatus used for current tests of combustng sprays appears in Fig. 3. The burner flow is injected vertically upward with combustion products removed at the ceiling of the test cell.

The flame is contained within a screened enclosure in order to minimize effects of room disturbances. Rigidly-mounted optical instrumentation is used for some measurements; therefore, the entire cage assembly is traversed for measurements of radial profiles.

The burner assembly has provision for stabilizing the flame and injecting drops of uniform size into the flow. A sketch of the arrangement appears in Fig. 4. The drops are formed using a commercial

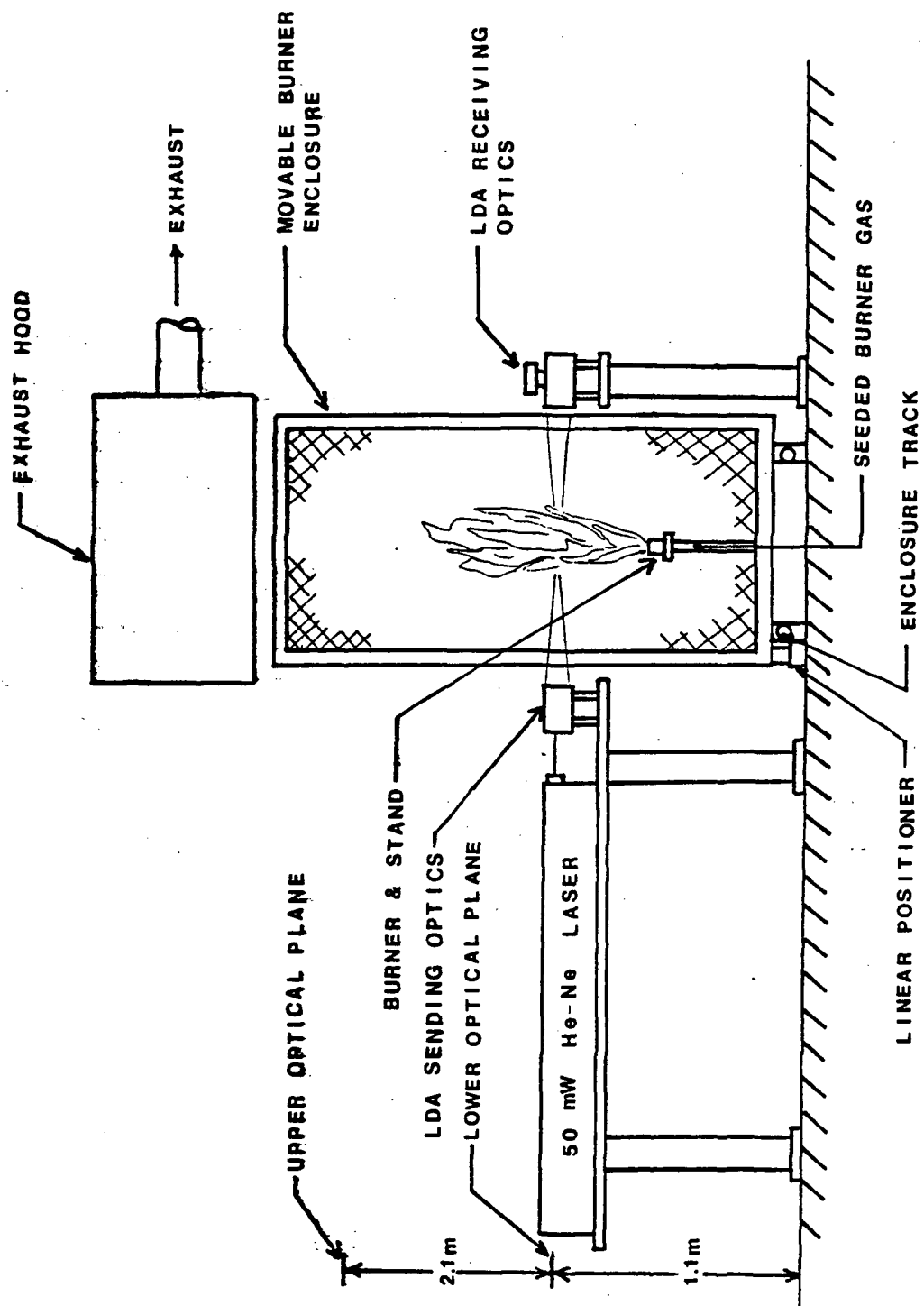


Fig. 3. Sketch of the combustng spray apparatus.

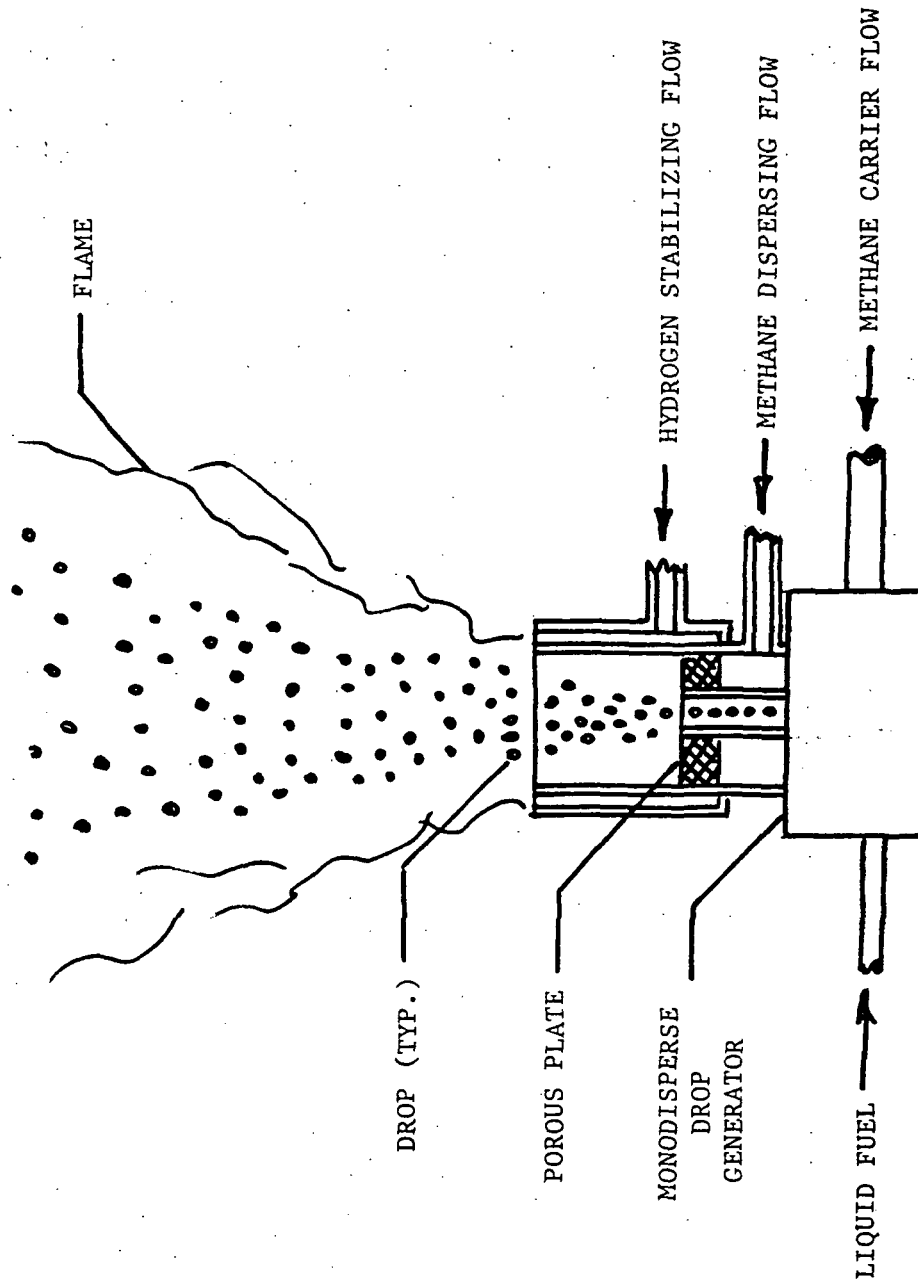


Fig. 4. Sketch of the monodisperse spray burner.

vibrating-orifice Berglund-Liu monodisperse drop generator (TSI model 3050). This generator is adjusted to provide drops having initial diameters of 100 and 180 microns.

In order to provide a fully turbulent flame having reasonable dimensions, the carrier and dispersing gas for the drop generator is natural gas. The combined drop/gas flame is attached at the burner exit using a hydrogen flame fueled from a narrow annular slot. The necessary hydrogen flow is small, on the order of 2.8% of the total fuel flow; therefore, the stabilizing flame has little effect on overall flame properties. The burner exit diameter is 5 mm, yielding a flame height (mean stoichiometric mixture ratio at the flame axis) of 400-600 mm for fully turbulent nonbuoyant conditions--excluding the effects of drops.

At first glance, using the same liquid fuel as the dispersing gas appears desirable. This is not really true for model evaluation purposes, however, since the degree of drop vaporization and the transport of vapor in the flame provides a critical test of predictions. Therefore, use of different liquid is preferred and methanol is used for the liquid fuel. It has a high heat of vaporization which extends the drop lifetime in the spray--simplifying measurements. Methanol combustion also yields minimal quantities of soot--minimizing problems of luminous flame radiation.

3.2 Instrumentation

Measurements include: phase velocities, drop sizes, drop fluxes and mean gas phase temperatures.

A laser Doppler anemometer (LDA) is used to measure mean and fluctuating gas velocities. Several beam orientations provide measurements of various velocity components as well as the Reynolds stress. The laser beams are frequency-shifted to eliminate errors due to fringe bias and flow reversal. Concentration biasing and effects of drops are avoided by employing high concentrations of seeding particles. Procedures generally follow practices that were successful for past work during this investigation [3-13].

Drop sizes are nearly uniform at each point in the flow, although they vary appreciably from point to point. therefore, the same arrangement is employed for drop velocity measurements without any need to distinguish drop sizes. In this case, no seeding particles are added to the flow and detector gain is reduced so that only relatively strong signals from drops are recorded. Drop velocity data is obtained as number averages since this quantity can be directly compared with predictions. The LDA output is stored and processed using a MINC 11/23 computer for this purpose.

Flash photography is used to measure drop sizes, with occasional use of double-flash photography to check LDA measurements of drop velocities. This involves photographing the flow under high magnification with one or two light flashes having short duration,

similar to past work [9-13]. In some regions of the flow, concentrations of drops are very low which would require an excessive number of photographs to accumulate a statistically significant sample. In these regions, slide impaction is used [9-13].

Drop fluxes are measured as a function of position using laser light scattering. This involves spreading a HeNe laser beam (50 mW) into a light sheet with a cylindrical lens and passing it through the flame. A small section of the sheet is observed with a photodetector. The output of the detector is processed with a pulse-height analyzer and counter. Knowing the area observed, the number of particle pulses and the time of sampling yields the drop number flux. This arrangement was checked using the slide impactor [9-13] and found to yield good results without the drudgery of counting drop craters on a slide.

The base methane flame is similar to the flame studied by Jeng and Faeth [22] so that complete structure measurements were not necessary. Current measurements of phase velocities and mean temperature were used to check for any major differences. The mean temperature measurements were made with a 50 micron diameter Pt/Pt 10% Rh thermocouple corrected for radiation errors, following past practice [22].

3.3 Drop-Life-History Calibrations

In order to assess unit transport process predictions of drops, tests were conducted for individual drop-life histories. This involved supporting drops from a quartz fiber and rapidly immersing them in the post-flame region of a flat-flame burner. The drops were backlighted and photographed, with timing marks placed on the film. Processing the photographs with an image analyzer then yielded drop size as a function of time.

The flat-flame burner was operated at various mixture ratios to yield a variety of conditions representative of flame environments. The burner design is the same as Szekely and Faeth [26,27]. Properties of the burner gases were measured by sampling and analysis with a gas chromatograph for composition and corrected fine-wire thermocouples for gas temperatures. Gas velocities were computed from the one-dimensional flow approximation, knowing the burner mass flow rate, the flow area and the density of the post-flame gases.

4. Results and Discussion

4.1 Drop-Life-History Calibrations

Flame conditions used for the drop-life-history tests are summarized in Table 1. Flame conditions are characterized by the fuel equivalence ratio, e.g., the fuel-air ratio divided by the stoichiometric fuel-air ratio.

The drop-life-history tests considered relatively large drops (2000-3000 micron initial diameter), in order to obtain drop Reynolds

Table 1. Summary of Drop-Life-History Test Conditions^a

Equivalence ratio	0.65	0.82	0.97
Flow temperature (k)	1500.	1690.	1690.
Initial drop diameter (μm)	2293.0	2786.0	2953.0
Drop Reynolds number	19.0	21.0	28.0
Species concentration (mass basis)			
O ₂	0.0758	0.0376	0.0002
N ₂	0.7552	0.7443	0.7782
H ₂ O	0.0771	0.0983	0.0991
CO	0.0042	0.0000	0.0011
CO ₂	0.0877	0.1198	0.1214

^aSupported methanol drops immersed in the post-flame region of a flat-flame burner fueled with methane-air mixture.

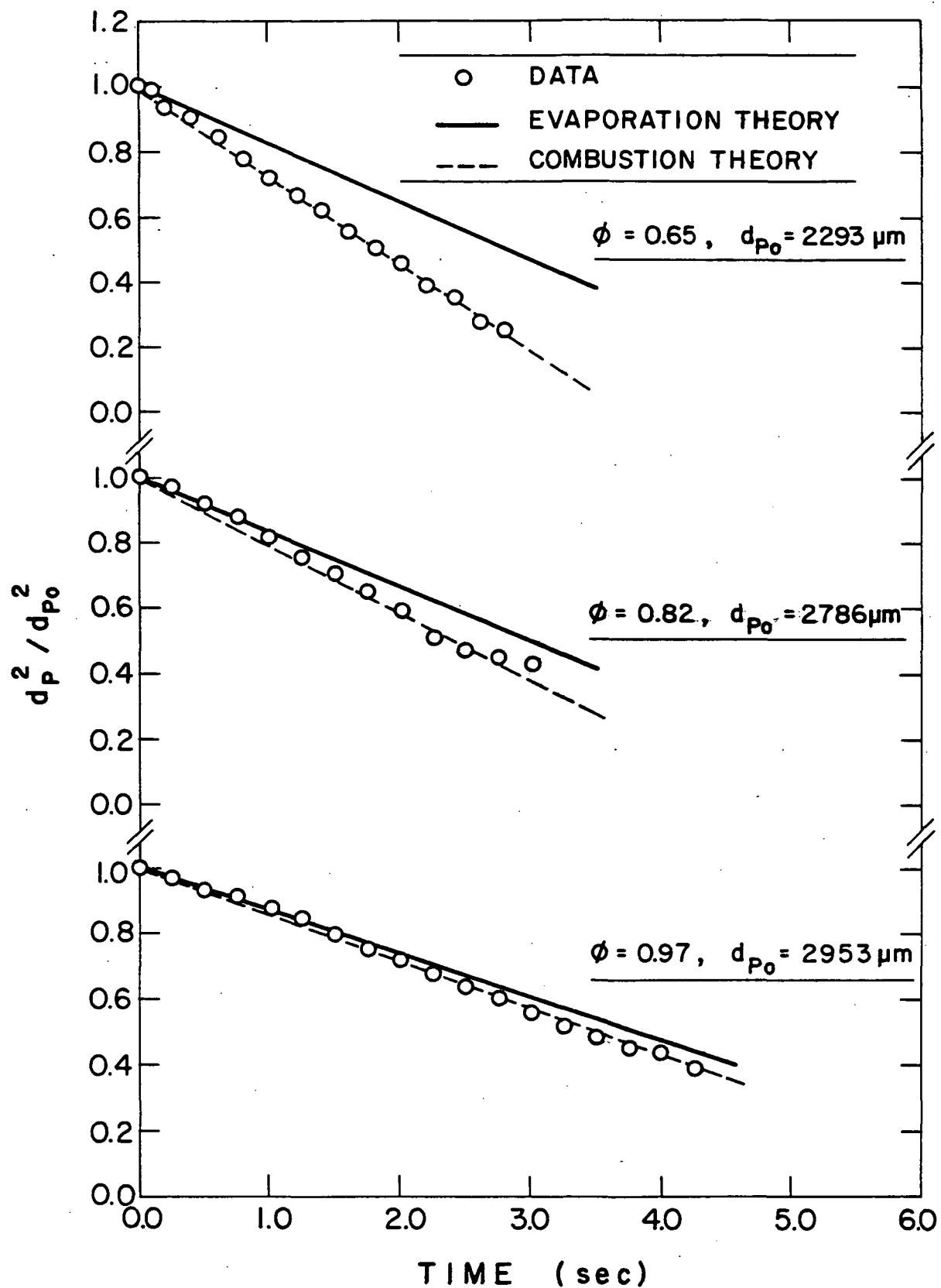


Fig. 5. Predicted and measured drop-life histories.

numbers representative of the turbulent flame conditions. The drop liquid was methanol. Predicted and measured drop-life histories are illustrated in Fig. 5 for flame fuel equivalence ratios of 0.97, 0.82 and 0.65. Predictions are shown for the limiting conditions of envelope flames present or absent--the latter condition representing simple drop evaporation. For both conditions predicted results are illustrated for $\alpha = 0.3$; where α is a reference parameter used to specify average conditions in the gas phase around the drop [1].

The results in Fig. 5 indicate that differences between predictions with and without envelope flames are not large for an equivalence ratio of 0.97 and are, of course, identical for equivalence ratios greater than unity. At lower fuel equivalence ratios, envelope flames must be considered for these conditions. However, smaller drop sizes and higher relative velocities in the turbulent flames still raise questions whether envelope flames will still be observed [1]. The best quantitative match between predictions and measurements is obtained using $\alpha = 0.3$; therefore, this selection completes the calibration for drop calculations under flame conditions.

4.2 Monodisperse Spray Structure

Testing is still in progress and initial conditions of the spray have not been measured completely; therefore, only a sample of the results obtained to date will be considered in the following. Burner operating conditions are summarized in Table 2.

Figure 6 is an illustration of predicted and measured flame temperatures along the axis. These conditions were measured with no drops being injected so that the results can be compared with earlier measurements by Jeng and Faeth [22]. Clearly, both sets of measurements are virtually identical, indicating excellent reproducibility of the earlier work. Predictions for this flame are in reasonably good agreement with the measurements, indicating that the analysis provides a reasonably good estimation of flame properties. In particular, earlier predictions of all scalar properties in this flame were reasonably satisfactory [22]. The sprays are sufficiently dilute so that spray operation causes only very small changes in flame properties.

Mean gas and drop velocities are illustrated in Fig. 7 for a monodisperse spray having an initial drop diameter of 180 microns. Predictions of gas properties are shown along with the measurements. This can be done since centerline properties of the spray have been measured at the burner exit. Gas velocities are substantially greater than drop velocities at the burner exit. However, gas velocities decay rapidly by mixing with the surroundings while the inertia of these relatively large drops maintains nearly a constant drop velocity over much of their lifetime; therefore, in the upper reaches of the flame, the drops move more rapidly than the gas. As the drops become small, near the end of their lifetime, they become more responsive so that mean drop and gas velocities are nearly equal in the upper reaches of the flow. Reference to Fig. 6 indicates that the maximum gas

Table 2. Burner Operating Conditions^a

<u>Gas Properties</u>		
Flow Rates (mg/s)		
Fuel ^b		520
Hydrogen		14.6
Initial Velocity ^c (m/s)		52.8
Reynolds Number ^d		11700
<u>Drop Properties</u>	<u>Case 1</u>	<u>Case 2</u>
Diameter (μm)	105	180
Liquid fuel flow rate ^e (mg/s)	4.82	19.34
Initial Velocity ^f (m/s)	15.0	11.9

^aBurner exit diameter = 5 mm.

^bNatural gas.

^cMeasured at centerline, $x/d = 1$.

^dBased on fuel gas properties and estimated velocity at burner exit.

^eMethanol, laboratory grade.

^fMeasured at centerline, $x/d = 1$.

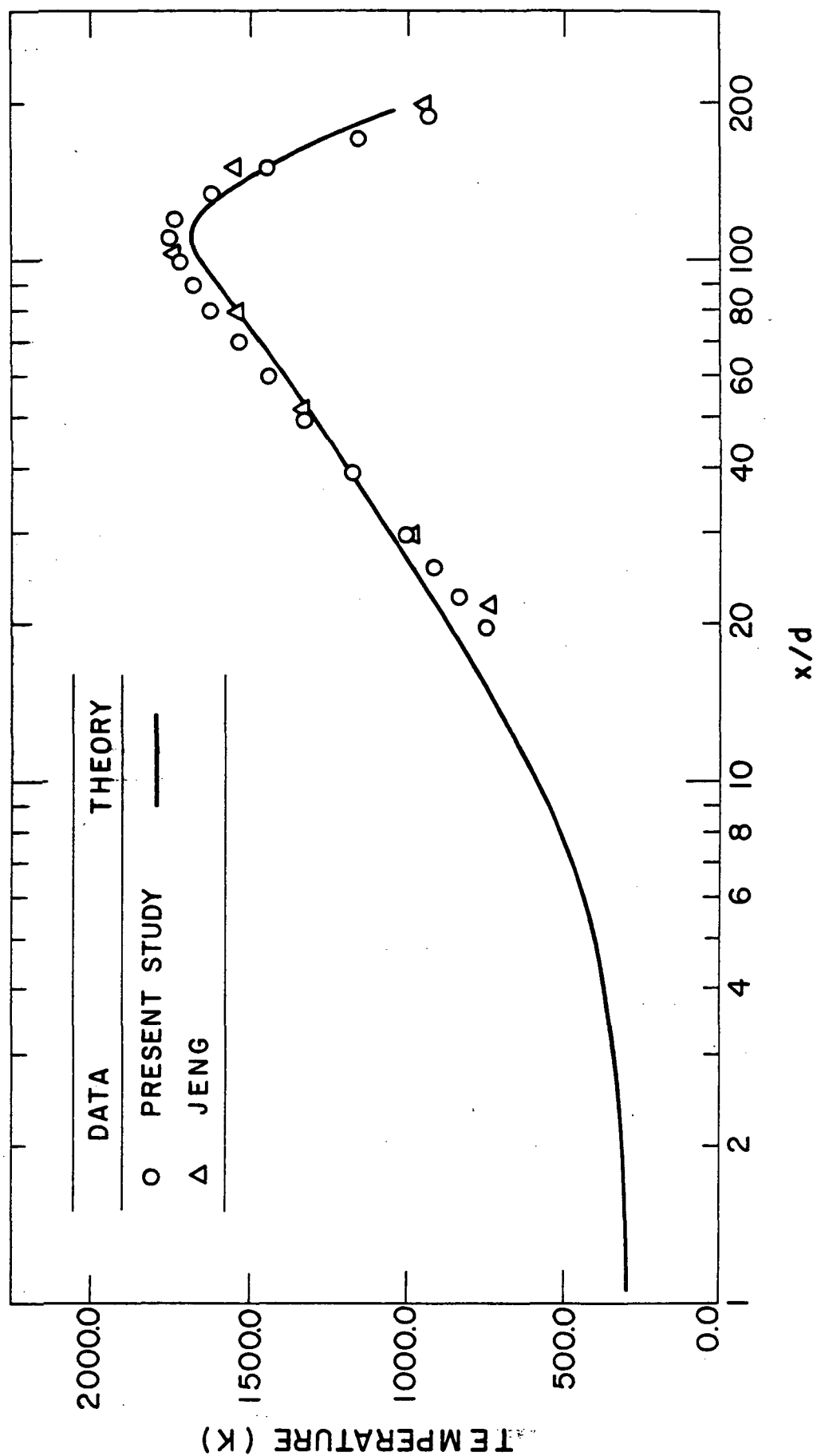


Fig. 6. Predicted and measured mean temperatures along the axis.

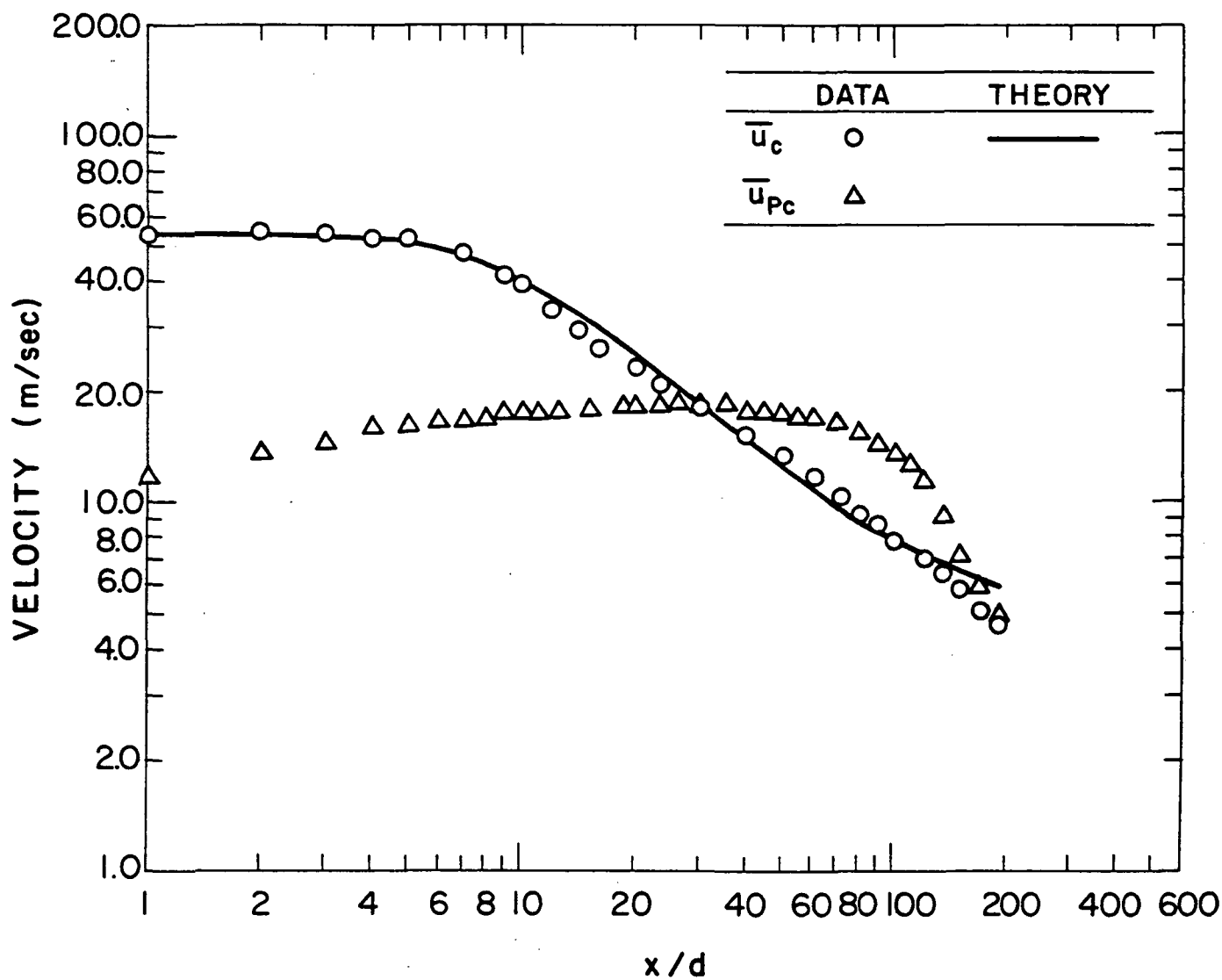


Fig. 7. Predicted and measured mean phase velocities along the axis, $d_{po} = 180$ microns.

temperature condition along the axis is reached near $x/d = 125$. This point also corresponds to the flame tip and appreciable concentrations of oxygen are present along the axis at positions farther downstream. The measurements in Fig. 7 show that drops penetrate beyond the flame tip (to about $x/d = 200$); therefore, these test results should indicate effects of the presence or absence of envelope flames.

Phase velocity fluctuations for the same spray are illustrated in Fig. 8. conditions near the injector are difficult to control in the experiment and are an artifact of the injection process. It happens that streamwise and radial velocity fluctuations of each phase are nearly identical at the burner exit, and are very nearly equal to each other. Moving away from the injector, however, both phases show increased levels of anisotropy--particularly the drop phase--with the streamwise velocity fluctuations being the greatest. Gas-phase velocity fluctuations increase rapidly near the end of the potential core, $x/d = 4-10$, cf., Fig. 7. This is generally observed in jet flames [22,23]: The streamwise velocity fluctuations of the drop phase respond somewhat to gas-phase fluctuations, but the levels are much lower due to drop inertia. This trend ends once the drops become small and their fluctuations rapidly increase to approach gas values. Of the three models being considered here, only the SSF approach has the potential to predict these trends. Therefore, this data should provide a challenging test of the SSF method.

Measured radial profiles of mean-drop velocities at $x/d = 20, 50$ and 100 are illustrated in Fig. 9. Data is plotted in terms of r/x , which is the similarity variable of fully-developed turbulent jets. Normalization of velocities tends to obscure effects of slip in these plots, but it is clear that drop velocities tend to be less responsive than gas velocities with increasing r/x , due to effects of drop inertia. Drop velocities are terminated when sampling rates become too low to obtain adequate statistics in a reasonable length of time. Clearly, these large drops are not being dispersed by turbulence to a great degree, which is expected due to their inertia.

Radial profiles of fluctuating-phase velocities for the same spray are illustrated in Fig. 10. Radial and tangential-phase velocity fluctuations are nearly identical, which is generally expected for jets. Streamwise gas-velocity fluctuations are somewhat greater than the other components, which is also typical of jets. The streamwise drop-velocity fluctuations are much greater than the other components, suggesting important effects of anisotropy. It will be most interesting to see if the SSF model can represent this trend.

5. Status and Plans for the Next Report Period

Crucial measurements of drop fluxes, drop sizes and initial conditions for the 180 micron spray are currently in progress. All measurements must be completed for the 100 micron spray as well. Finally, computations must be completed for all test conditions and

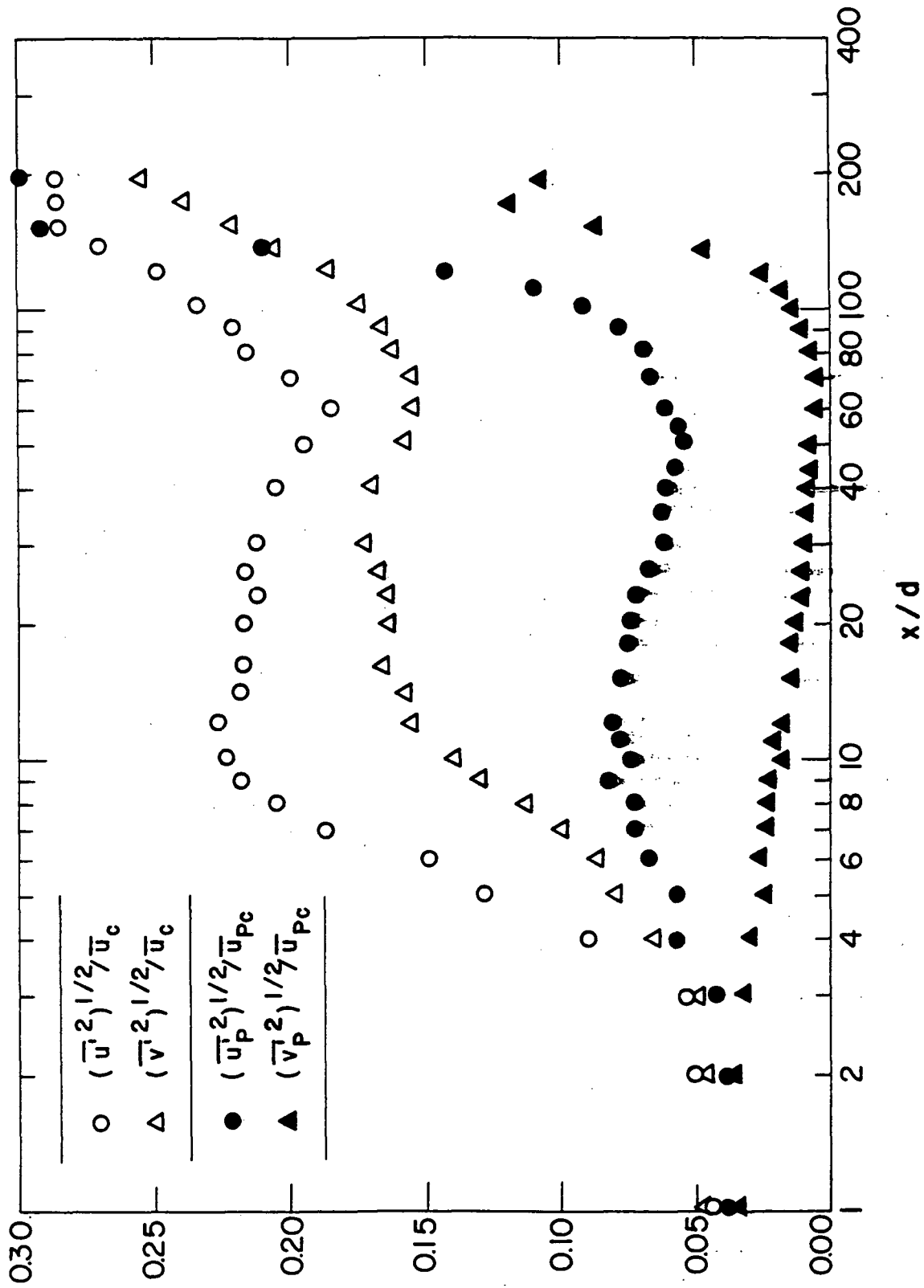


Fig. 8. Phase velocity fluctuations along the axis, $d_{po} = 180$ microns.

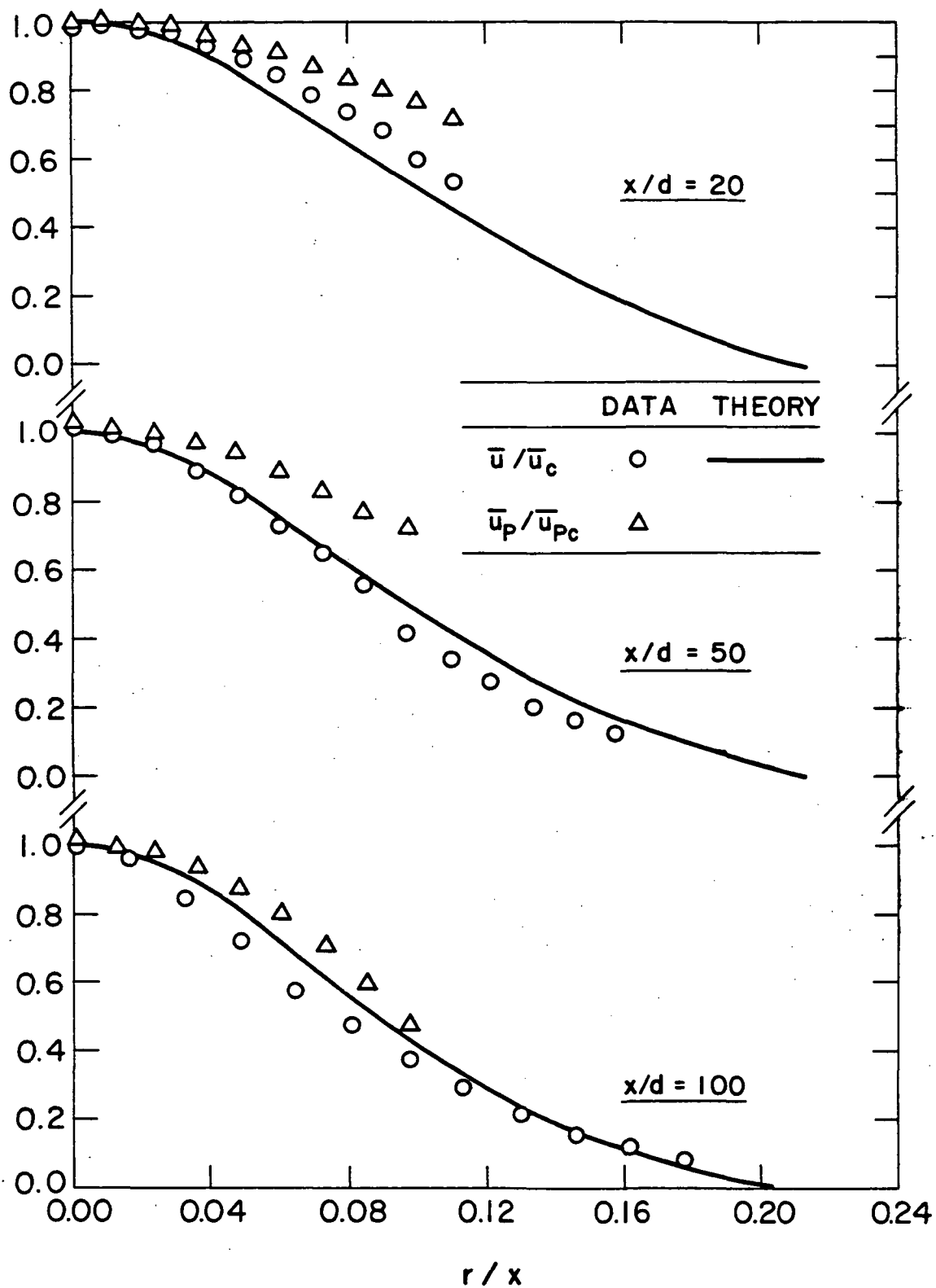


Fig. 9. Radial profiles of mean phase velocities, $d_{po} = 180$ microns.

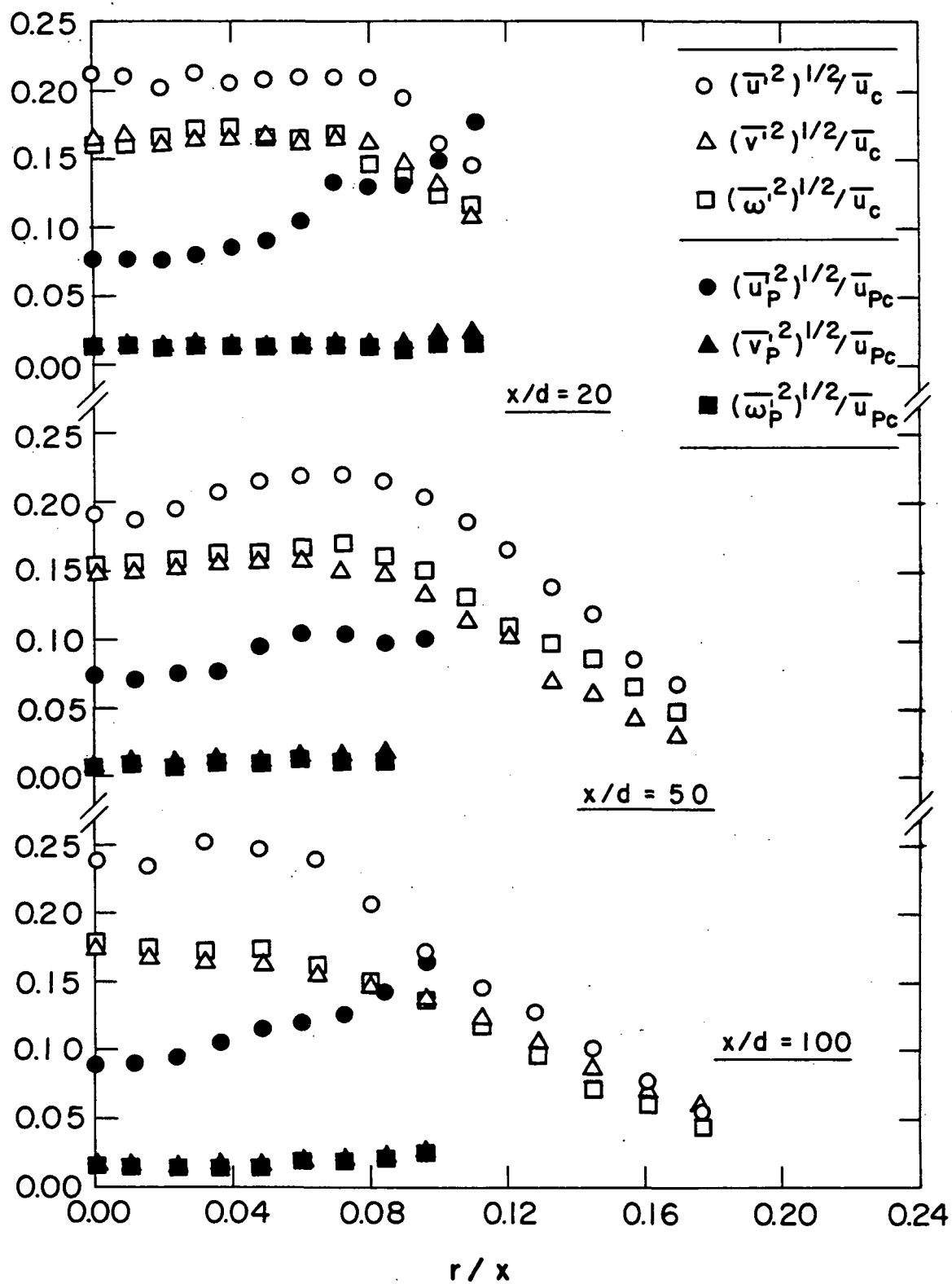


Fig. 10. Radial profiles of fluctuating phase velocities, $d_{po} = 180$ microns.

models. As time permits, it would be desirable to consider a third spray having smaller drops.

The results being obtained from the monodisperse spray burner are proving to be most interesting in disclosing properties of dilute sprays. Therefore, we plan to concentrate our efforts on results with this apparatus in order to exploit it to the full extent possible. As a result, tests using the air-atomizing injector will not be undertaken, since this represents a substantial measuring task which would be more appropriate after results for the simpler monodisperse burner are in hand.

REFERENCES

1. Faeth, G. M., "Evaporation and Combustion of Sprays," Prog. in Energy and Combust. Sci., 1984.
2. Faeth, G. M., "Recent Advances in Modeling Particle Transport Properties and Dispersion in Turbulent Flow," Proceedings of the ASME-JSME Thermal Engineering Conference, Vol. 2, ASME, New York City, 1983, pp. 517-534.
3. Shuen, J.-S., Solomon, A.S.P., Zhang, Q.-F. and Faeth, G. M., "The Structure of Particle-Laden Jets and Nonevaporating Sprays," NASA Contractor Report 168059, 1983.
4. Shuen, J.-S., Chen, L.-D. and Faeth, G. M., "Evaluation of a Stochastic Model of Particle Dispersion in a Turbulent Round Jet," AIChE J., Vol. 29, 1983, pp. 167-170.
5. Shuen, J.-S., Chen, L.-D. and Faeth, G. M., "Predictions of the Structure of Turbulent, Particle-Laden Jets," AIAA Paper No. 83-0066, 1983; also AIAA J., Vol. 21, 1983, pp. 1483-1484.
6. Solomon, A.S.P., Shuen, J.-S., Zhang, Q.-F. and Faeth, G. M., "Measurements and Predictions for Nonevaporating Sprays in a Quiescent Environment," AIAA Paper No. 83-0151, 1983.
7. Shuen, J.-S., Solomon, A.S.P., Zhang, Q.-F. and Faeth, G. M., "Structure of Particle-Laden Jets: Measurements and Predictions," AIAA Paper No. 84-0038, 1984; also, AIAA J., in press, 1984.
8. Shuen, J.-S., Solomon, A.S.P., Zhang, Q.-F. and Faeth, G. M., "A Theoretical and Experimental Study of Turbulent Particle-Laden Jets," NASA CR-168293, 1983.
9. Solomon, A.S.P., Shuen, J.-S., Zhang, Q.-F. and Faeth, G. M., "Structure of Nonevaporating Sprays: Measurements and Predictions," AIAA Paper No. 84-0125, 1984.
10. Solomon, A.S.P., Shuen, J.-S., Zhang, Q.-F. and Faeth, G. M., "Structure of Nonevaporating Sprays: I. Near-Injector Conditions and Mean Properties; II. Drop and Turbulence Properties," submitted to AIAA J., 1984.
11. Solomon, A.S.P., Shuen, J.-S., Zhang, Q.-F. and Faeth, G. M., "A Theoretical and Experimental Study of Turbulent Nonevaporating Sprays," Report under NASA Grant NAG 3-190, The Pennsylvania State University, 1984.
12. Solomon, A.S.P., Shuen, J.-S., Zhang, Q.-F. and Faeth, G. M., "Measurements and Predictions of the Structure of Evaporating Sprays," 22nd ASME/AIChE. National Heat Transfer Conf., August 1984; also submitted to J. Heat Transfer, 1984.

13. Solomon, A.S.P., Shuen, J.-S., Zhang, Q.-F. and Faeth, G. M., "A Theoretical and Experimental Study of Turbulent Evaporating Sprays," Report under Grant NAG 3-190, 1984.
14. Shearer, A. J., Tamura, H. and Faeth, G. M., "Evaluation of a Locally Homogeneous Flow Model of Spray Evaporation," J. of Energy, Vol. 3, September-October 1979, pp. 271-278.
15. Mao, C.-P., Szekely, G. A., Jr. and Faeth, G. M., "Evaluation of a Locally Homogeneous Flow Model of Spray Combustion," J. of Energy, Vol. 4, March-April 1980, pp. 78-87.
16. Mao, C.-P., Wakamatsu, Y. and Faeth, G. M., "A Simplified Model of High Pressure Spray Combustion," Eighteenth Symposium (International) on Combustion, The Combustion Institute, Pittsburgh, 1981, pp. 337-347.
17. Lockwood, F. C. and Naguib, A. S., "The Prediction of the Fluctuations in the Properties of Free, Round-Jet, Turbulent, Diffusion Flames," Combustion and Flame, Vol. 24, 1975, pp. 109-124.
18. Bilger, R. W., "Turbulent Jet Diffusion Flames," Prog. Energy combust. Sci., Vol. 1, 1976, pp. 87-109.
19. Jeng, S.-M., Chen, L.-D. and Faeth, G. M., "The Structure of Buoyant Methane and Propane Diffusion Flames," Nineteenth Symposium (International) on combustion, The Combustion Institute, Pittsburgh, 1982, pp. 1077-1085.
20. Bilger, R. W., "Reaction Rates in Diffusion Flames," Combustion and Flame, Vol. 30, 1977, pp. 277-284.
21. Liew, S. K., Bray, K.N.C. and Moss, J. B., "A Flamelet Model of Turbulent Non-Premixed Combustion," Comb. Sci. and Tech., Vol. 27, 1981, pp. 69-73.
22. Jeng, S.-M. and Faeth, G. M., "Species Concentrations and Turbulence Properties in Buoyant Methane Diffusion Flames," J. Heat Trans., in press.
23. Jeng, S.-M. and Faeth, G. M., "Predictions of Mean and Scalar Properties in Turbulent Propane Diffusion Flames," J. Heat Trans., in press.
24. Szekely, G. A., Jr. and Faeth, G. M., "Effects of Envelope Flames on Drop Gasification Rates in Turbulent Diffusion Flames," Comb. Flame, Vol. 11, 1983, pp. 255-259.
25. Gosman, A. D. and Ioannides, E., "Aspects of Computer Simulation of Liquid-Fueled Combustors," AIAA Paper No. 81-0323, 1981.

26. Szekely, G. A., Jr. and Faeth, G. M., "Reaction of Carbon Black Slurry Agglomerates in Combustion Gases," Nineteenth Symposium (International) on Combustion, The Combustion Institute, Pittsburgh, 1982, pp. 1077-1085.
27. Szekely, G. A., Jr. and Faeth, G. M., "Effects of Carbon-Black Properties on Combustion of Carbon-Black Slurry Agglomerates," submitted to Combustion and Flame.